

dent study of the satellite multiplet as a function of temperature is now in progress. The much shorter FID's of the central transition produced by increased second-order quadrupole broadening at lower temperatures will be likely to require the application of a third pulse (at ν_1) in order to use a quadrupole echo¹⁴ for data acquisition.

We hope that the proposed interferometric technique will be useful as a simple and sensitive tool for investigation of quadrupole interactions in half-integer spin systems. It allows the simultaneous measurements of both first- and second-order quadrupolar energy shifts and, thus, is capable of unraveling spectra complicated by several overlapping $\frac{1}{2} \leftrightarrow -\frac{1}{2}$ transitions (including powder patterns) and chemical-shift anisotropies. In particular, since the first- and second-order quadrupolar energies are averaged differently by atomic motions, the proposed scheme can furnish additional information concerning dynamical phenomena in solids.

We are most grateful for the valuable advice and assistance of Dr. A. J. Vega and Albert Highe and wish to acknowledge financial support from the U. S. Energy Research and Development Administration (Contract No. EY-76-S-03-0767) for performance of this work. The apparatus used was funded in part by an equipment grant from

the National Science Foundation.

¹M. E. Stoll, A. J. Vega, and R. W. Vaughan, *Phys. Rev. A* **16**, 1521 (1977).

²M. E. Stoll, A. J. Vega, and R. W. Vaughan, *J. Chem. Phys.* **67**, 2029 (1977).

³M. H. Cohen and F. Reif, in *Solid State Physics*, edited by Frederick Seitz, Henry Ehrenreich, and David Turnbull (Academic, New York, 1957), Vol. 4, p. 321.

⁴*Superionic Conductors*, edited by G. D. Mahan and W. L. Roth (Plenum, New York, 1976).

⁵R. E. Walstedt, R. Dupree, J. P. Remeika, and A. Rodriguez, *Phys. Rev. B* **15**, 3442 (1977).

⁶W. Bailey, S. Glowinkowski, H. Story, and W. L. Roth, *J. Chem. Phys.* **64**, 4126 (1976).

⁷I. Chung, H. S. Story, and W. L. Roth, *J. Chem. Phys.* **63**, 4903 (1975).

⁸J. P. Boilot, L. Zuppiroli, G. Delphanque, and L. Jerome, *Philos. Mag.* **32**, 343 (1975).

⁹H. S. Story, unpublished private communication, has observed a single narrow (5–15 kHz) line which seems to behave as a fully averaged satellite.

¹⁰The β -alumina crystal was cut from a boule supplied by Union Carbide, Crystal Products Division, and should be comparable to that used in Refs. 4–7.

¹¹M. Polak and R. W. Vaughan, to be published.

¹²R. V. Pound, *Phys. Rev.* **79**, 685 (1950).

¹³H. Hatanaka, T. Terao, and T. Hashi, *J. Phys. Soc. Jpn.* **39**, 835 (1975).

¹⁴A. Abragam, *The Principles of Nuclear Magnetism* (Oxford Univ. Press, London, 1961), pp. 241–246.

Band Structure of AlAs-GaAs(100) Superlattices

J. N. Schulman and T. C. McGill

California Institute of Technology, Pasadena, California 91125

(Received 13 July 1977)

We report the results of the first band-structure calculation for AlAs-GaAs superlattice structures consisting of several atomic monolayers of AlAs and GaAs per repeated slab. The tight-binding method is used to investigate the band gaps and the character of the electronic states as a function of the number of monolayers per slab. For any fixed concentration of Al, the material becomes direct as the number of monolayers per slab is increased. The states at the band edges are predominantly in the GaAs layers and die away into the AlAs.

Recently, molecular-beam epitaxy techniques have been used to fabricate heterostructures consisting of alternating slabs of AlAs and GaAs.^{1,2} Up to now, the spectra have been analyzed by approximating the layered system as being a series of GaAs wells sandwiched between larger-band-gap AlAs barriers.^{4–6} Variations on the one-dimensional Kronig-Penney model with bulk-related effective masses and potential barriers cho-

sen to duplicate the optical spectra⁴ have been used. Very recently Caruthers and Lin-Chung⁷ have reported on a non-self-consistent, empirical pseudopotential calculation of the band structure of alternating *single* layers of GaAs and an alloy of $\text{Ga}_{1-x}\text{Al}_x\text{As}$. Their calculations for GaAs on AlAs have the feature of producing states such that the energy gap would be 1.58 eV. This result is in direct disagreement with the photolumi-

nescence and absorption data which both give about 2 eV for this gap.¹

In this Letter we report the first results of a parametrized tight-binding calculation, which takes account of the three-dimensional atomistic details of the material. The calculation is done for several systems, each having alternating slabs made up of various numbers of AlAs and GaAs layers.

The main results obtained are the band structure and band-gap variation as a function of the AlAs and GaAs slab thicknesses, and the character of the states at the band edges. In addition to giving a description of the superlattice structure, this method can also be used to investigate the electronic properties of the AlAs-GaAs interface in the limit in which the slab thicknesses become large. Interface states, having wave functions localized within a few monolayers of the interface, can then be identified.

This calculation assumes a perfect lattice match-up and abrupt interface between the two compounds.⁸ The standard three-dimensional tight-binding formalism can be applied to this situation with one modification. The conventional fcc unit cell of the zinc-blende crystal must be enlarged in the direction perpendicular to the (100) interface in order to include one complete slab each of AlAs and GaAs. This enlarged unit cell is then repeated indefinitely in all three directions thus forming the complete crystal. There are interfaces dividing each unit cell in two as well as interfaces at the boundaries between cells.

The tight-binding basis wave functions used were one *s*-type orbital and three *p*-type (p_x , p_y , and p_z) orbitals per anion and per cation. Letting M and N equal the number of AlAs and GaAs layers per slab, respectively, there will be a total of $(M+N) \times 8$ basis functions per unit cell. The Hamiltonian matrix will have $[(M+N) \times 8]^2$ elements and will be of a general form similar to that used by Hirabayashi.⁹ The repeating slab structure is dealt with by including matrix elements between the first and last monolayers of the slab.

The AlAs and GaAs tight-binding parameters used here were found by separately fitting them to recent bulk pseudopotential calculations.^{10,11} Some second-nearest-neighbor parameters were necessary to reproduce roughly the shape of the lowest conduction band in both AlAs and GaAs. Even so, these parameters incorrectly give the GaAs indirect gap as being between X and K in-

stead of at L . The Al-Ga second-nearest-neighbor matrix-element parameters were taken to be the average of the corresponding Al-Al and Ga-Ga parameters. Since the calculation is not self-consistent we are unable to determine the band discontinuities or charge-transfer differences between the Al and Ga. However, the electronegativities for Al and Ga are very similar ($\Delta\chi=0.02$ on the Phillips scale).¹² Computation of the layer charge densities show that charge transfer occurs only at the interface layer and is small for these layers. In the wide, separated-well limit, Dingle, Wiegmann, and Henry⁴ fit optical data with a valence-band discontinuity equal to about 15% of the direct-gap differences between GaAs and $\text{Ga}_{1-x}\text{Al}_x\text{As}$. We used their results and thus subtracted this valence-band discontinuity from the four AlAs diagonal bulk parameters. The number of independent parameters was reduced by using the two-center approximation of Slater and Koster.¹³ The parameters are given in their notation in Table I.

Since the superlattice has the ordinary zinc-blende periodicity in the two directions parallel to the AlAs-GaAs interface, there is a two-dimensional reciprocal lattice with a square Brillouin zone as shown in the inset to Fig. 1. Each point in this reciprocal space has mapped onto it $M+N$ points of the three-dimensional bulk zinc-blende reciprocal space. Figure 1 shows the band structure from Γ to J for the superlattice consisting of two layers of AlAs alternating with two layers of GaAs ($M=2, N=2$). There are a total of 32 bands (ignoring degeneracy). The energy bands for \vec{k} perpendicular to the layers are not shown here. The dispersion for the highest valence band is about 0.2 eV and for the lowest conduction band about 0.1 eV. Both curve in such a way as to increase the band gap.

Conduction-band-edge energies relative to the top of the valence band were calculated for several fixed ratios of M to N . The energies were calculated at two reciprocal-lattice points, Γ and J . The Γ point represents the direct gap, and J has the bulk L point mapped onto or near it,¹⁴ the GaAs bulk reciprocal-lattice point with the experimentally lowest indirect gap. It is found that even when the material is indirect, the band-edge states are mostly on the GaAs ions. Therefore, it is the J point which determines whether the material is direct or indirect. The AlAs bulk conduction-band minimum is at the bulk X point which maps onto the two-dimensional Brillouin-zone Γ point. Figure 2 shows the results for up to twelve

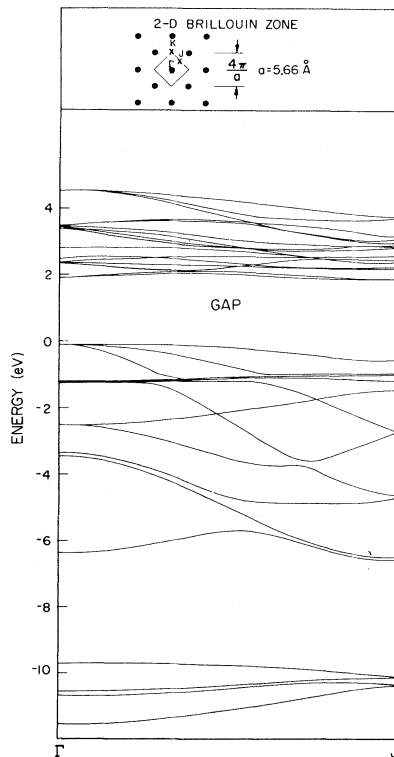


FIG. 1. Band structure of the AlAs-GaAs superlattice consisting of two monolayers of AlAs alternating with two monolayers of GaAs from Γ to J . The inset shows the two-dimensional Brillouin zone. The magnitude of \vec{k} at the J point is $(\sqrt{2}\pi/a)$ with $a = 5.66 \text{ \AA}$.

monolayers of GaAs per slab. It is seen that for $x \lesssim 0.4$ [$x \equiv M/(M+N)$], the material is always direct. The alloy $\text{Ga}_{1-x}\text{Al}_x\text{As}$ goes from being direct to indirect for $x \gtrsim 0.4$. The superlattice, however, can still be direct if it has a large enough number of GaAs layers per slab. For $x = 0.5$ the superlattice is direct if $N \geq 3$, and for $x = 0.67$ it is direct if $N \geq 4$. For small numbers of layers per slab, the Γ -point conduction-band-edge energy is increased over its bulk GaAs value more than the J -point energy. As M and N increase for any ratio, Γ and J approach their bulk values.

The character of the states was found from the eigenvectors of the tight-binding matrix. The results shown in Fig. 3 are typical for the band-edge states. It shows the charge distribution over the eight layers making up the repeated slab for the case $M=N=4$ at two energies—the top of the valence band and the bottom of the conduction band. The states are heavily concentrated on the GaAs part of the slab as is true for all the super-

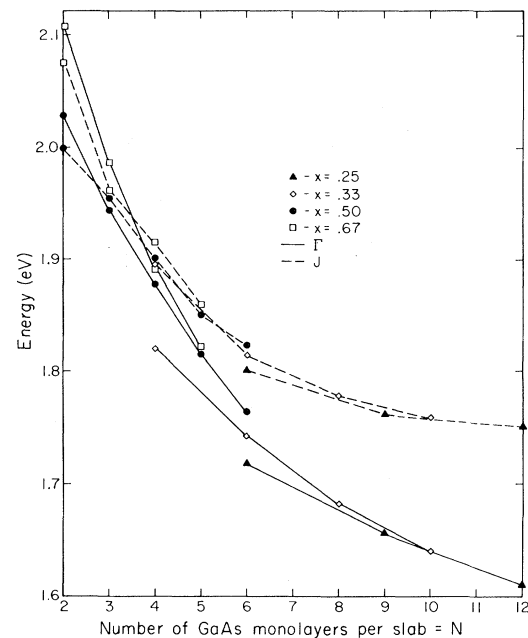


FIG. 2. The energy gaps between the top of the valence band and the lowest Γ and J point in the conduction band versus number of GaAs layers, N , in the superlattice. A number of different superlattices are shown. The number of AlAs layers, M , in a superlattice $(\text{AlAs})_M(\text{GaAs})_N$ is given by $M = xN/(1-x)$, that is, x is the relative fractional Al concentration in the superlattice.

lattices investigated. The ratios of total Ga to As squared amplitudes are very similar to the corresponding ratios found from diagonalizing the bulk GaAs tight-binding matrix, showing that these superlattice states are derived from the GaAs band-edge states. No states which were localized near the AlAs-GaAs interfaces were found with energies within the band gap.

The experimental studies of optical properties of superlattices¹ give values of the band gap in good agreement with our theoretical calculations. For $N=M=1$, the experimental absorption edge is found to be at about 2 eV. Extrapolating our $N=M$ results to $N=1$ gives a value slightly greater than 2 eV.¹⁵ For $M=3$ and $N=6$, our calculated direct gap is 1.74 eV which compares well with the measured value of somewhat greater than 1.8 eV.

In conclusion, it is found that both the energy-gap behavior and the character of the electronic states indicate that the band-edge states are closely related to the corresponding bulk GaAs states. These calculations support the claim that the superlattices are significantly different from

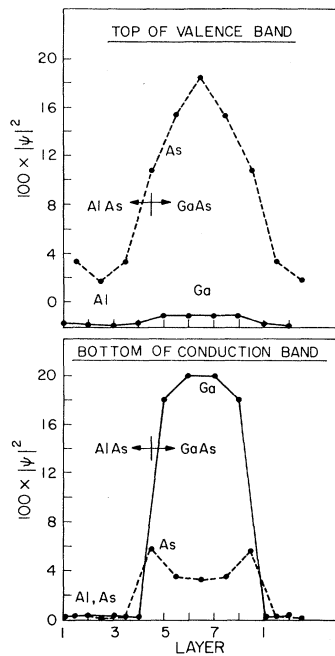


FIG. 3. Anion (As) and cation (Al and Ga) charge distributions for a superlattice consisting of four layers of AlAs alternating with four layers of GaAs. The dotted line is for the anion and the solid line for the cation.

the corresponding alloys.¹ Further, they suggest that it may be possible to fabricate superlattices with technically interesting optical properties. For example, GaAs/AlAs superlattices may be formed that have both a direct edge and an energy gap greater than that obtainable in the direct-band-gap alloys. A more detailed publication including density of states per layer is in preparation.

The authors wish to acknowledge many useful discussions with D. L. Smith. This work was supported in part by the U. S. Office of Naval Research under Contract No. N00014-76-C-1068 and in part by the Army Research Office under Contract No. DAAG29-77-C-0015. One of us (T.C.M.) acknowledges receipt of a fellowship from the Alfred P. Sloan Foundation.

¹A. C. Gossard, P. M. Petroff, W. Wiegmann, R. Dingle, and A. Savage, *Appl. Phys. Lett.* **29**, 323 (1976).

²L. L. Chang, L. Esaki, W. E. Howard, R. Ludeke, and G. Schul, *J. Vac. Sci. Technol.* **10**, 655 (1973).

³J. P. van der Ziel and A. C. Gossard, to be published.

⁴R. Dingle, W. Wiegmann, and C. H. Henry, *Phys. Rev. Lett.* **33**, 827 (1974).

⁵L. Esaki, L. L. Chang, W. E. Howard and V. L. Rideout, in *Proceedings of the Eleventh International Conference on the Physics of Semiconductors, Warsaw,*

TABLE I. Tight-binding parameters for AlAs and GaAs determined by fitting to bulk pseudopotential calculations. The notation is that of Ref. 13. The subscripts 0 and 1 designate anion and cation, respectively. All parameters are given in units of eV.

	AlAs	GaAs
$E_{ss}(000)_0$	-9.288	-9.227
$E_{ss}(000)_1$	0.328	-0.263
$E_{xx}(000)_0$	-1.851	-1.534
$E_{xx}(000)_1$	2.521	1.659
$E_{ss}(1/2, 1/2, 1/2)$	-1.418	-1.091
$E_{xx}(1/2, 1/2, 1/2)$	0.175	0.264
$E_{xy}(1/2, 1/2, 1/2)$	0.418	0.620
$E_{sx}(1/2, 1/2, 1/2)_{01}$	0.531	0.662
$E_{sx}(1/2, 1/2, 1/2)_{10}$	0.799	0.974
$E_{xx}(011)_0$	-0.074	-0.159
$E_{xx}(011)_1$	0.144	0.365
$E_{xy}(110)_0$	0.323	0.461
$E_{xy}(110)_1$	-0.004	-0.197
$E_{xx}(110)_0$	0.249	0.302
$E_{xx}(110)_1$	0.140	0.168

Poland, 1972 (Elsevier, Amsterdam, 1972), Vol. 1, p. 431.

⁶D. Mukherji and B. R. Nag, *Phys. Rev. B* **12**, 4338 (1975).

⁷E. Caruthers and P. J. Lin-Chung, *Phys. Rev. Lett.* **38**, 1543 (1977).

⁸Both materials are zinc-blende. The cubic lattice constants are 5.654 Å for GaAs and 5.661 Å for AlAs [see A. C. Milnes and D. L. Feucht, *Heterojunctions and Metal Semiconductor Junctions* (Academic, New York, 1972), p. 8].

⁹K. Hirabayashi, *J. Phys. Soc. Jpn.* **27**, 1475 (1969).

¹⁰E. Hess, I. Topol, K. R. Schulze, H. Neumann, and K. Unger, *Phys. Status Solidi (b)* **55**, 187 (1973).

¹¹J. R. Chelikowsky and M. L. Cohen, *Phys. Rev. B* **14**, 556 (1976).

¹²J. C. Phillips, *Bonds and Bands in Semiconductors* (Academic, New York, 1973), p. 54; L. Pauling, *The Nature of the Chemical Bond* (Cornell Univ. Press, Ithaca, N.Y., 1960), 3rd ed., p. 93.

¹³J. C. Slater and G. F. Koster, *Phys. Rev.* **94**, 1498 (1954).

¹⁴When the total number of layers per slab is odd, a small reciprocal-lattice vector perpendicular to the two-dimensional reciprocal lattice must be added to J in order to include the bulk L point. Since the size of this vector is small [$\pi/(M+N)a$], the difference in energy of the point in k space where the L point is mapped and the J point is only a few millivolts.

¹⁵We have not made calculations for $M=N=1$. The existence of overlap matrix elements between electronic states centered on adjacent layers necessitates a slight modification of our program for this case. We will report on the results of this calculation in a future publication.